Annual Review of Marine Science

The Hydrodynamics of Jellyfish Swimming

John H. Costello,[1] Sean P. Colin,[2] John O. Dabiri,[3] Brad J. Gemmell,[4] Kelsey N. Lucas,[5] and Kelly R. Sutherland[6]

[1]Department of Biology, Providence College, Providence, Rhode Island 02918, USA; email: costello@providence.edu

[2]Department of Marine Biology and Environmental Science, Roger Williams University, Bristol, Rhode Island 02809, USA; email: scolin@rwu.edu

[3]Graduate Aerospace Laboratories and Department of Mechanical and Civil Engineering, California Institute of Technology, Pasadena, California 91125, USA; email: jodabiri@caltech.edu

[4]Department of Integrative Biology, University of South Florida, Tampa, Florida 33620, USA; email: bgemmell@usf.edu

[5]School for Environment and Sustainability, University of Michigan, Ann Arbor, Michigan 48109, USA; email: kelsey.n.lucas@gmail.com

[6]Oregon Institute of Marine Biology, University of Oregon, Eugene, Oregon 97403, USA; email: ksuth@uoregon.edu

Annu. Rev. Mar. Sci. 2021. 13:5.1–5.22

The *Annual Review of Marine Science* is online at marine.annualreviews.org

https://doi.org/10.1146/annurev-marine-031120-091442

Keywords

propulsion, biomechanics, biomimetic, zooplankton, rowing propulsion

Abstract

Jellyfish have provided insight into important components of animal propulsion, such as suction thrust, passive energy recapture, vortex wall effects, and the rotational mechanics of turning. These traits are critically important to jellyfish because they must propel themselves despite severe limitations on force production imposed by rudimentary cnidarian muscular structures. Consequently, jellyfish swimming can occur only by careful orchestration of fluid interactions. Yet these mechanics may be more broadly instructive because they also characterize processes shared with other animal swimmers, whose structural and neurological complexity can obscure these interactions. In comparison with other animal models, the structural simplicity, comparative energetic efficiency, and ease of use in laboratory experimentation allow jellyfish to serve as favorable test subjects for exploration of the hydrodynamic bases of animal propulsion. These same attributes also make jellyfish valuable models for insight into biomimetic or bioinspired engineering

of swimming vehicles. Here, we review advances in understanding of propulsive mechanics derived from jellyfish models as a pathway toward the application of animal mechanics to vehicle designs.

INTRODUCTION

Cnidarian medusae, more commonly known as jellyfish, are one group among a variety of animal models that provide insight for novel propulsive systems. Two attributes uniquely position jellyfish among these models: First, the energetic efficiency of swimming scyphomedusae is among the highest for all animal swimmers (**Figure 1**), and, second, their mechanical design requires the most limited set of structural components among muscle-powered animal swimmers (Costello et al. 2008). Quantification of fluid interactions involving jellyfish is further aided by their physical organization: The transparent or translucent nature of their gelatinous bodies often enables ready visualization through their body tissues, and their axisymmetric, radial body architecture provides a substantial benefit for extrapolation of two-dimensional measurements to the full three-dimensional body shape (Gemmell et al. 2015a,b). The pulsatile nature of their swimming can also contribute to high hydrodynamic efficiency (Ruiz et al. 2011, Whittlesey & Dabiri 2013). Additionally, many jellyfish, particularly the genus *Aurelia* (moon jellies), are easily reared through multiple size stages ranging from viscous through inertial flows that allow for testing of scale-dependent effects (Feitl et al. 2009, Higgins et al. 2008, McHenry & Jed 2003, Nagata et al. 2016, Nawroth et al. 2010), and because members of this genus are circumglobal, they are commonly

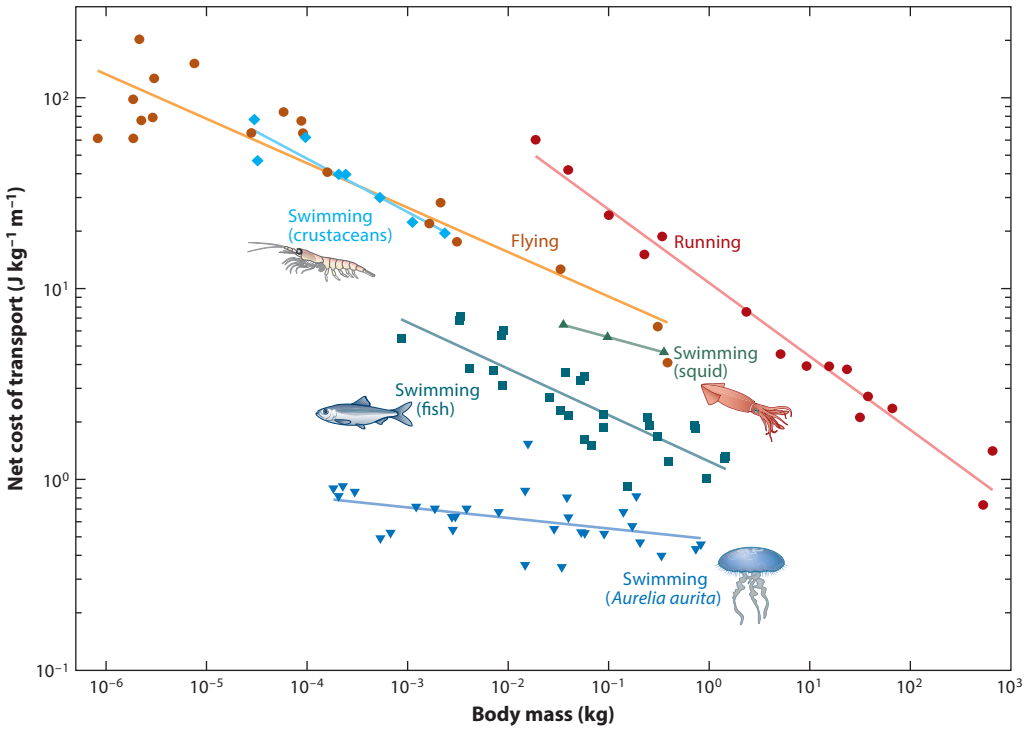

Figure 1

Net cost of transport for swimming, flying, and running animals relative to body mass. Swimmers are separated into crustaceans, squid, fish, and the jellyfish *Aurelia aurita*. Figure adapted with permission from Gemmell et al. (2013).

BIOMIMETIC UNDERWATER VEHICLES

Conventional underwater vehicles rely on propellers for propulsion, which are hydrodynamically noisy and inefficient and often lack the maneuverability and efficiency of swimming animals. The need for better underwater vehicles has prompted work to design biomimetic or bioinspired underwater vehicles that are capable of "swimming" as well as, or better than, animals. Much of this research has used fish models (Jusufi et al. 2017, Kim et al. 2017); however, the simplicity and efficiency of jellyfish propulsion may be ideal for applications that require long-term vehicle deployments (Joshi et al. 2019, Villanueva et al. 2009).

available. This combination—high efficiency, low complexity, and ready availability—is appealing for energy-limited underwater vehicle applications that do not require high velocities (see the sidebar titled Biomimetic Underwater Vehicles).

From a biological perspective, the energetic efficiency of jellyfish models is a direct consequence of the evolutionary constraints on the material design of these animals (Costello et al. 2008). Cnidaria possess one of the most limited arrays of cellular building blocks within the animal kingdom from which to construct operable swimming designs. Both the neurological (Satterlie 2002, 2011, 2015) and mechanical (Bonner 1965, Chapman 1974) systems of cnidarians are comparatively limited relative to those of most other metazoan phyla. The long evolutionary history of jellyfish has selected for high energetic efficiency as a prerequisite for their limited mechanical components to permit swimming. In other words, these animals had to be highly efficient, because otherwise their very limited body components would have been insufficient to power swimming (Dabiri et al. 2007, McHenry 2007). Documentation of the fluid interactions that allow successful thrust production by jellyfish has allowed identification of essential hydrodynamic mechanisms that may be shared by a range of animal swimmers with more complex body forms, such as swimmers possessing multiple fins and other propulsive surfaces (Fish & Lauder 2017). However, for the purposes of determining hydrodynamic interactions underlying efficient vehicle design, jellyfish are highly instructive models with a long history of ready access through laboratory culture.

Here, we review advances in our understanding of propulsion that have arisen from empirical quantification of swimming medusae. Although these studies all have a modeling component, the patterns reviewed here are based primarily on empirical laboratory studies. We recognize the important advantages of computational fluid dynamic descriptions and other modeling approaches for formalizing critical relationships among variables. These approaches have enabled pattern predictions over a range of conditions that are often impractical or impossible for direct empirical quantification with animals or vehicles (Dular et al. 2009; Hoover et al. 2017, 2019; Lipinski & Mohseni 2009; Miles & Battista 2019; Park et al. 2014). These studies have demonstrated the importance of the animal kinematics (i.e., movements) that underlie fluid dynamic patterns. The most pronounced success of computational fluid dynamic models has come when incorporating detailed biological information (e.g., Gemmell et al. 2013, Hoover et al. 2017) rather than relying on assumed kinematic or material traits.

The empirically based experimental work reviewed in this article details previously undescribed physical processes that underlie the success of jellyfish propulsion. The novelty of these processes (e.g., suction thrust, passive energy recapture, wall effects, and rotational dynamics) is not a result of their extreme complexity. In retrospect, these findings may seem more obvious than novel because, once documented, they appear straightforward. However, their documentation required the development of new, nonintrusive methods for high-resolution measurement of forces along the animal bodies moving through fluids (Dabiri et al. 2014, Gemmell et al. 2015a, Lucas et al. 2017).

PARTICLE IMAGE VELOCIMETRY

Particle image velocimetry (PIV) is a technique used to quantify the hydrodynamics around aquatic animals. Most common PIV systems use a laser to illuminate a two-dimensional sheet of water that has been seeded with tiny reflective particles. When an animal swims through the laser sheet, video images of the particle movements can be captured and analyzed. PIV software uses a cross-correlation algorithm to convert the movement of the particles illuminated in the two-dimensional sheet to velocity vectors. These velocity vectors are the basis of other important hydrodynamic quantities, such as kinetic energy, pressure, and force. Three-dimensional systems also exist that use multiple cameras to measure the three-dimensional movement of particles.

These methods, similarly to those used in a variety of propulsion studies (e.g., Drucker & Lauder 2000, Quinn et al. 2014, Tytell & Lauder 2004), utilize particle image velocimetry techniques (Willert & Gharib 1991) (see the sidebar titled Particle Image Velocimetry). However, rather than evaluating average traits of fluid motions downstream in the wake of swimmers (Floryan et al. 2019), the dynamics we describe depend on the measurement of instantaneous forces along a swimmer's body while it alters body configurations in the fluid.

The capability of direct force and torque measurement during swimming has provided new insights about previously undocumented propulsive mechanisms. The ideal marriage of these new insights with advanced modeling approaches has the potential to enable a range of innovation in understanding propulsion of both animals and vehicles. Our purpose here is to contribute to this potential by assembling highlights of recent empirical work that may serve to enable propulsive innovation in vehicles inspired by jellyfish (Frame et al. 2018; Najem et al. 2012; Nawroth et al. 2012; Ren et al. 2019; Villanueva et al. 2011; Xu & Dabiri 2020; Yu et al. 2016, 2019) or, potentially, by other organisms that share common mechanics (Dabiri et al. 2019).

BIOLOGICAL BACKGROUND: WHAT EXACTLY ARE JELLYFISH?

All medusae are members of the animal phylum Cnidaria. More specifically, they are part of the taxon Medusazoa, a division within the Cnidaria composed primarily of lineages that produce medusae as some component of their life cycle. However, as a group, medusae are diverse in size, shape, coloniality, body design, and propulsive mode (**Figure 2**). Their functional variety has been examined in detail (Costello et al. 2008), but most of the research on medusan propulsion has focused on one group—the scyphomedusae. This group contains the largest individual medusae (as much as 2 m in bell diameter), and the members are commonly referred to as jellyfish. The term jellyfish has no actual systematic validity but has gained widespread acceptance, and we use it here to refer specifically to scyphomedusae. One genus among the scyphomedusae, the semaeostome *Aurelia*, has received the most attention for hydrodynamic studies and is the most frequent model of jellyfish swimming.

MECHANICAL DESIGN: HOW ARE JELLYFISH CONSTRUCTED?

An idealized jellyfish body resembles a hemispherical bell (**Figure 3**). The underside of the curved hemisphere, or subumbrellar cavity, is continuous with the exterior fluid environment. Jet-propelled hydromedusae possess a thin flap of elastic tissue, termed the velum, surrounding the aperture. Likewise, jet-propelled cubomedusae possess an analogous constricting structure called the velarium. Swimming via jet propulsion involves contraction of circular muscle fibers lining the subumbrellar surface (which are therefore termed subumbrellar muscles). Shortening

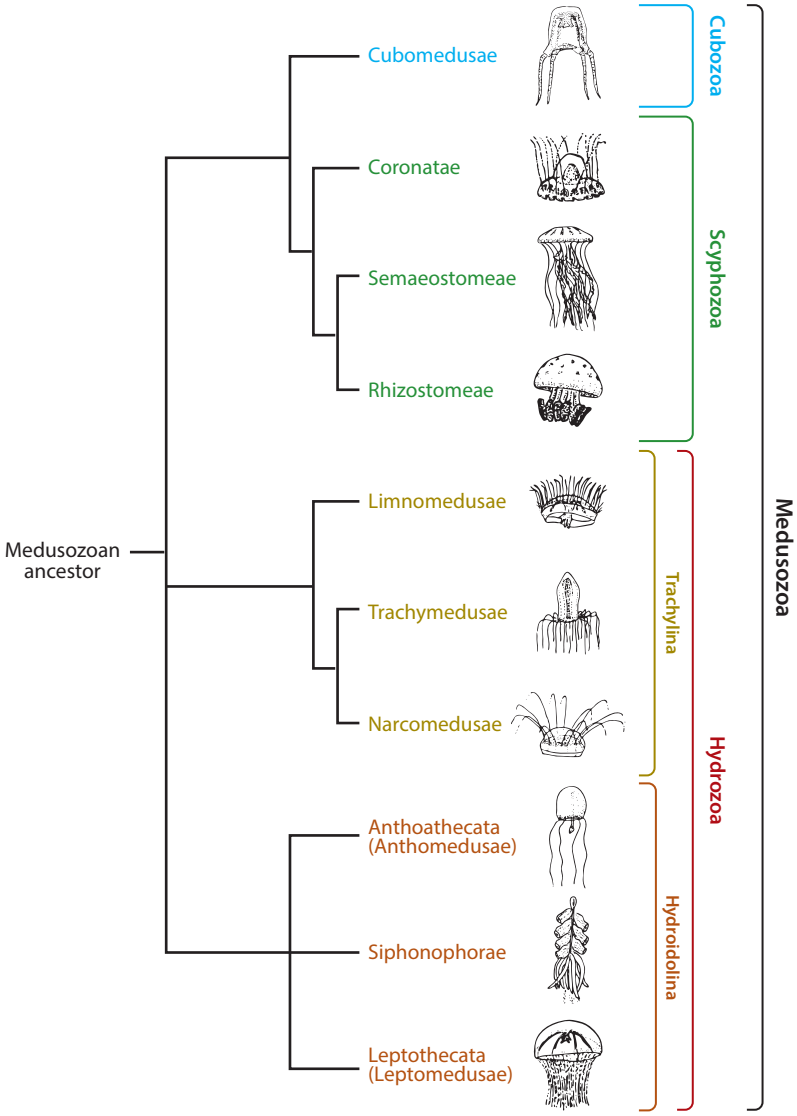

Figure 2

Medusan diversity, illustrating phylogenetic hypotheses based on work by Collins et al. (2006). Only extant (or non-extinct) lineages containing medusae are shown. Parenthetical lineage names reflect historical nomenclature when referring to the medusan portions of life cycles, rather than the current systematic nomenclature. Figure adapted with permission from Costello et al. (2008).

of the subumbrella muscles contracts the bell and reduces the subumbrellar volume. This action forces fluid out of the subumbrellar region either as a series of vortices (scyphomedusae) or as a jet through the velar aperture (hydromedusae). Simultaneously, the force of the exiting jet produces thrust and propels the medusa forward (Costello et al. 2019; Dabiri et al. 2005, 2006; Daniel 1983; Gemmell et al. 2015a).

Prolate: elongated or bullet-shaped in form; prolate jellyfish typically produce a jet of water during swimming

In contrast to that idealized jet-propelled model characterizing prolate medusae, scyphomedusae do not possess a velum or velarium to direct a jet of fluid during bell contraction. Instead,

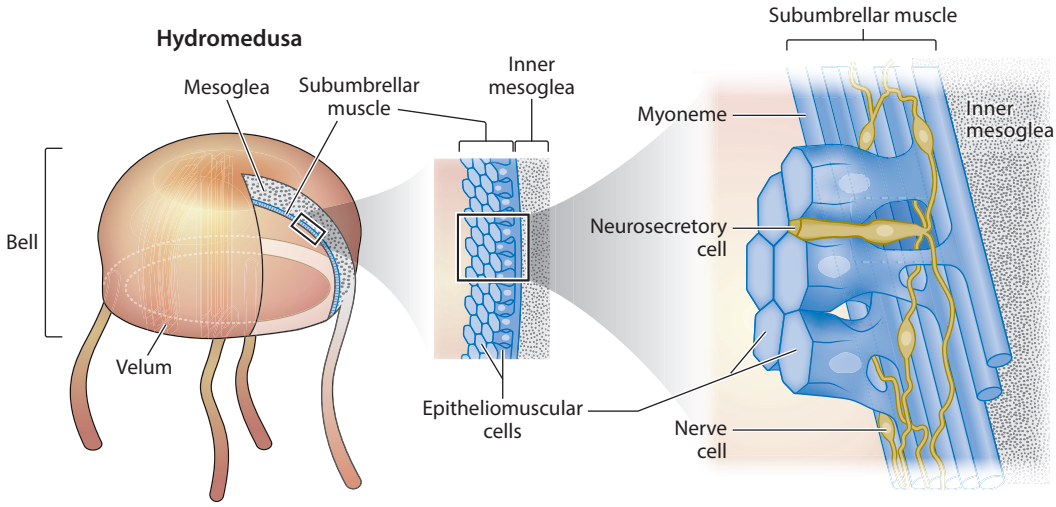

Figure 3

Hydromedusan swimming bell and muscle fiber structures. The major force for bell contraction is derived from contraction by the subumbrellar muscle sheet that is arranged with fibers oriented around the circumference (termed either circumferential or circular muscle fibers) of the bell. Bell relaxation occurs when the muscle fibers cease contracting and elastic strain stored during contraction by fibers within the mesoglea acts antagonistically to return the bell to its original, relaxed shape. Hydromedusae possess a velum, as depicted here, but scyphomedusae do not, and their subumbrellar cavity is open to the surrounding fluid. Figure adapted with permission from Costello et al. (2008).

scyphomedusan jellyfish are more oblate in form, resembling a curved plate, and move fluids both inside and outside their bells during the bell pulsation cycle to achieve high propulsive efficiency. This requires fine control of the bell margin (**Figure 4**), and recent research has demonstrated that there are subumbrellar fibers in a radial direction (Gemmell et al. 2015b, Zimmerman et al. 2019). Radial muscle fibers are oriented from the bell center toward the margin, essentially perpendicular to the circular muscles (**Figure 4*b*,*c***). Contraction of the radial fibers allows the bell margin to deform differentially around the bell during the broader circular muscle contraction of the power stroke of bell pulsation. This ability to control the deformation of the bell margin is important for vortex manipulation at the bell margin.

Oblate: plate-shaped in form; oblate jellyfish predominantly use paddling motions (termed rowing) to move water around the bell margin during swimming

Striated muscle: muscle tissue with repeating bands of fibers and striped appearance

JELLYFISH MUSCLE STRUCTURE AND BELL ACTUATION

The force that the subumbrellar muscles can produce is directly related to the pressure that expels fluid out of the subumbrellar cavity (DeMont & Gosline 1988a). Subsequently, the subumbrellar muscles relax, and the bell returns to its original relaxed form due to antagonistic interactions of elastic fibers within the mesoglea of the medusan bell (Megill et al. 2005). Bell relaxation is accompanied by refilling of the subumbrellar cavity with fluid. Bell contraction is generally more rapid than bell relaxation, and the asymmetry in the timing of the two phases results in greater fluid velocities, and hence momentum, during bell contraction than during bell relaxation. As a result of cyclic bell contraction and relaxation, swimming by medusae involves pulsed, unsteady motion (Daniel 1983).

The structure and function of medusan muscular contraction provides a mechanism that may limit the range of bell shapes possible at larger bell diameters (Costello et al. 2008, Dabiri et al. 2007). Medusan subumbrellar muscular tissues share many traits with striated muscles that are involved in motion of most other metazoans. From a molecular perspective, sequence analysis

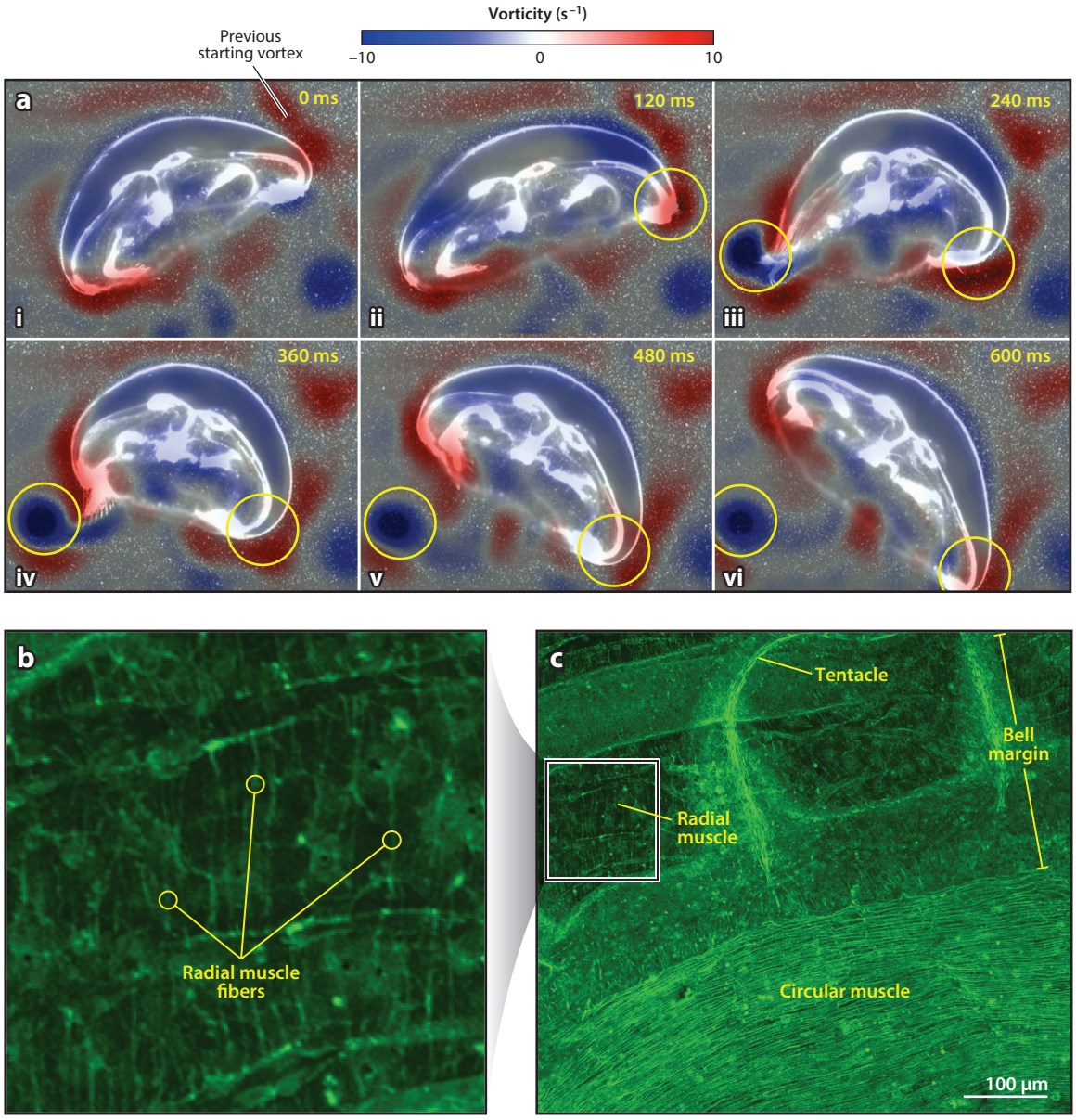

Figure 4

Maneuvering by the jellyfish *Aurelia aurita*. (*a*) Planar particle imaging velocimetry sequence showing vorticity generation relative to body position, with the starting vortices circled in yellow. Note that the starting vortex on the inside of the turn (*red*) remains in close proximity to the body, while the starting vortex on the outside of the turn (*blue*) separates from the bell. (*b*) High-magnification view showing the loose array of radial muscle fibers in the bell margin. (*c*) Actin staining of *Aurelia* muscle showing both the bell (with circular muscle) and bell margin. Figure adapted with permission from Gemmell et al. (2015b).

Myofibril: an elongated contractile thread that makes up striated muscles

Sarcomere: the structural unit of striated muscle myofibrils

of muscle-specific myosin heavy-chain genes, from striated muscle fibers of the hydromedusa *Podocoryne carnea* Sars 1846, strongly resemble the striated muscle tissues of bilateral animals (Seipel & Schmid 2005). Structurally, medusan subumbrellar myofibrils show a banding structure similar to that of vertebrate skeletal muscles (Boelsterli 1977, Schuchert et al. 1993), and the sarcomere lengths of medusan subumbrellar myofibrils (2–3 μm) (Chapman 1974) are similar to those of vertebrate skeletal muscles (2.0–2.8 μm) (Biewener & Patek 2018). Sarcomere length is generally related to force production (Biewener & Patek 2018, Vogel 2013), and the maximum isometric stress estimates of medusan subumbrellar muscles (0.13–0.20 N mm^{-2}) (Bone & Trueman 1982, DeMont & Gosline 1988b) are of a magnitude similar to those of frog and rat leg muscles (0.15–0.36 N mm^{-2}) (Alexander 2003). The molecular, structural, and functional similarities between medusan striated muscle fibers and those of higher metazoans suggest that force production patterns of medusan swimming muscle tissue may resemble those of higher metazoan striated muscles.

However, despite these similarities, jellyfish subumbrellar muscle tissues are organized in a fundamentally different pattern from the striated muscles used for movement in other animal phyla. The most important distinction involves the epithelial nature of cnidarian muscular tissues. The myocytes of most animal muscle tissues are elongated, multinucleate entities that are highly specialized for muscular contraction and, along with enervating motor neurons, are bundled into motor units of variable thickness and length. Although the dynamics of contractions differ among muscle types (Alexander 2003, Biewener & Patek 2018), the conservative nature of actin and myosin in striated muscles of a variety of animal phyla results in force generation that is relatively similar per unit of muscle cross-sectional area. Consequently, thicker layers of muscle fibers typically generate greater total force (Biewener & Patek 2018). In contrast to the striated myocytes of most metazoans, medusan subumbrellar myofibrils are restricted to epithelial cells termed epitheliomuscular cells (**Figure 3**). These cells are typically cylindrical or squamous in shape, and myofibrils are located in the basal portion of the cell only (**Figure 3**). Most importantly, the epitheliomuscular cells lining the medusan subumbrellar surface are only one cell thick. Consequently, the myofibrils available to generate force for bell contraction are limited in depth, and hence cross-sectional area, to this single cell layer.

An exceptional case of muscle fibers combining to form fascicles has been described for cubomedusan tentacles (Simmons & Satterlie 2018) but not for cubomedusan bells or for any other medusan lineage. For most medusae, bundles of myofibrils formed at the basal ends of epitheliomuscular cells encircle the subumbrellar cavity, and it is the contraction of these circularly oriented muscle fibers that reduces bell volume and produces swimming thrust (Gladfelter 1973). The myofibrils of even large, muscular scyphomedusan jellyfish, such as *Cyanea capillata*, are thin (3.5 μm) (Gladfelter 1972). The subumbrellar myofibrillar sheet of some scyphomedusan jellyfish may be folded and interlocked with the mesogleal region (Anderson & Schwab 1981, Gladfelter 1972), thereby contributing a secondary means of increasing muscle cross-sectional area. Such folding can result in an approximately fivefold increase in the effective cross-sectional area of myoepithelial tissues (Gladfelter 1972). The restriction of striated myofibrils to epithelial cells is a cnidarian trait (Chapman 1974), and the limited cross-sectional area of subumbrellar epitheliomuscular tissues represents an important phylogenetic constraint on force production by swimming medusae.

FORCE PRODUCTION AND BELL DIMENSIONS

The constrained architecture of medusan subumbrellar actuation critically influences size-dependent patterns of medusan bell morphology. The muscular contractile forces required to

achieve jet propulsion do not scale favorably with increasing medusa size for several reasons. The major reason is that, for an idealized hemispherical hydromedusa, muscular capacity for force generation increases as a linear function of bell diameter. This is because muscle fiber depth is phylogenetically constrained to one cell layer, and the muscular cross-sectional area is then only proportional to the circumference of the subumbrellar cavity. By contrast, the hydrodynamic force requirements for accelerating the mass of fluid in a jet used for propulsion increase as a cubic function of bell diameter because the accelerated fluid depends on the volume of the subumbrellar cavity. Hence, the force required for jet propulsion increases with animal size more rapidly than the available physiological force. A similar force-scaling pattern dictates the upper limit on the size of squid, another animal known to use jet propulsion (O'Dor & Hoar 2000, Pauly 1997).

An additional reason why contractile forces do not scale favorably with size is that the pressure in the subumbrellar cavity that is used to expel the fluid jet is caused by tension in the bell due to muscle contraction. However, in accordance with Laplace's law, the amount of pressure created per unit bell tension decreases with increasing bell diameter (for a sphere, pressure = tension/radius). The amount of force available for jet production is further diminished because only a portion of the force generated by contraction of the subumbrellar muscle sheet is available to generate hydrostatic pressure on the subumbrellar fluid and generate a fluid jet. A substantial fraction does not directly impact fluid jet production (Demont & Gosline 1988b, Megill et al. 2005) but is instead stored as elastic recoil energy within the mesoglea. One consequence of jellyfish muscular structure is that force production for bell actuation is strongly limited.

Suction thrust: the thrust created by low-pressure suction on the forward-facing surface of a jellyfish's bell margin; this suction results from flow generated during bell contraction and pulls the body forward

Passive energy recapture (PER): the use of elevated pressure along a jellyfish's inner bell surface; this pressure is generated by a stopping vortex ring during bell refilling after contraction and pushes the body forward

Wall effect: the generation of greater pressure and thrust by a virtual wall underneath the medusa that is created by the stopping vortex produced during the prior pulse

THE HYDRODYNAMIC BASIS OF HIGH-EFFICIENCY TRANSLATION BY JELLYFISH

If jellyfish have such limited force production capabilities, then how can they be such efficient swimmers? The answer lies with how jellyfish move the body components they do have—otherwise known as bell kinematics. Jellyfish propulsive efficiency depends on bell kinematics that generate three critical components: suction thrust during bell contraction, passive energy recapture (PER) following bell relaxation, and a wall effect boost that occurs during contractions following an initial bell contraction. While integral to the pulsed nature of jellyfish swimming, these components occur during different phases of the pulsation cycle (**Figure 5**).

Suction Thrust

Suction thrust is the dominant source of jellyfish propulsive thrust. During bell contraction, the flexible bell margins of jellyfish create counterrotating vortices along the outside of the bell margin. At the interface between these vortices, fluid is accelerated, creating a high-velocity, low-pressure region on the forward-facing surface of the bell margin (Colin et al. 2012, Dabiri et al. 2019). This low pressure surrounding the forward surface of the bell generates a suction force that pulls the medusa forward (**Figure 6*a–d***). Simultaneously, water propelled backward by the contracting bell creates a high-pressure region that pushes the medusa forward. The push forces have long been identified in medusan swimming; the pull or suction thrust component has only recently been quantified (Colin et al. 2012, Gemmell et al. 2015a) yet is the dominant contributor to net forward thrust (**Figure 6*e*,*f***). The pressure differential across the bell margin surface is dependent on vortex structures generated by the contracting bell margin and is the reason that flexible, bending margins are critical to achieve the high efficiency of jellyfish propulsion (Colin et al. 2012).

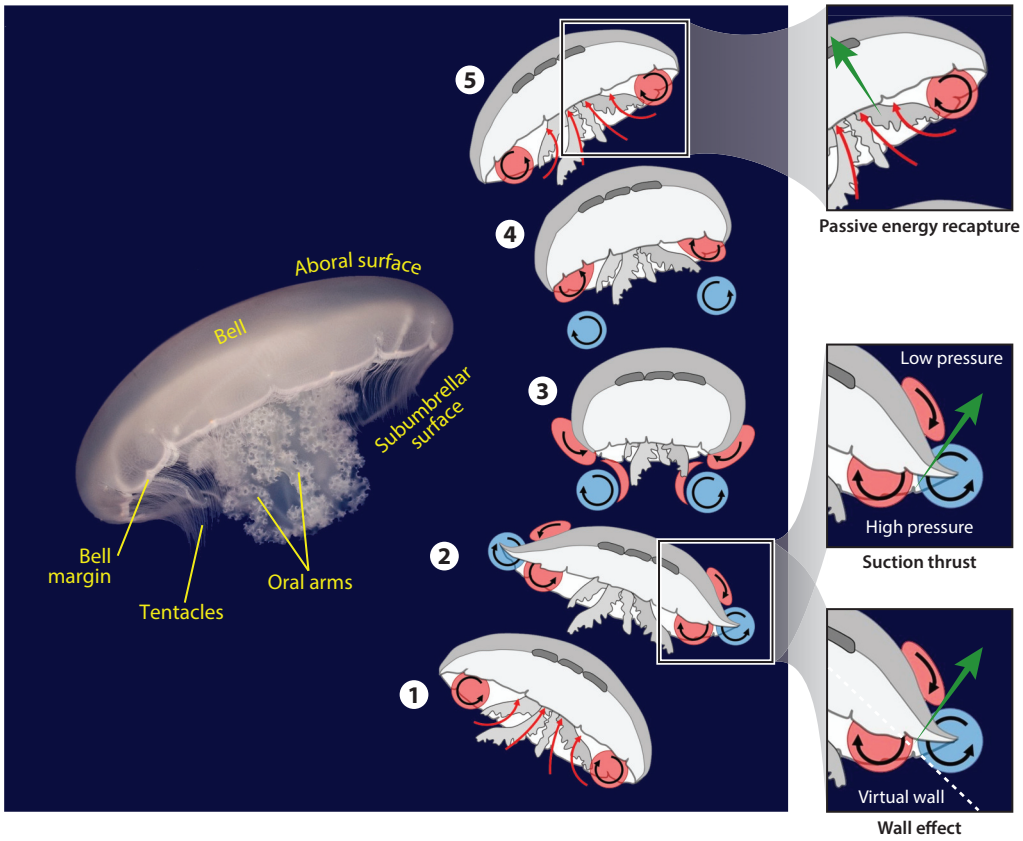

Figure 5

Jellyfish (*Aurelia* spp.) anatomy and critical vortex interactions allowing efficient jellyfish swimming. Red areas represent stopping vortices, and blue areas represent starting vortices. Black arrows denote the direction of fluid circulation. Green arrows represent the direction of thrust contribution provided by the different vortex interactions. (①) During the relaxation phase of a pulsation cycle, a stopping vortex resides within the subumbrellar cavity and induces flow upward against the subumbrellar surface in a process known as passive energy recapture (Gemmell et al. 2013). (②) The bell margin bends, forming a vortex at the aboral surface. This vortex creates a pressure gradient across the bell margin that results in suction thrust along a high-to-low pressure gradient (Colin et al. 2012, Gemmell et al. 2015a). There is also vortex–vortex interaction underneath the bell that creates a virtual wall effect (Gemmell et al. 2020). (③) As the starting vortex is pushed away from the bell margin, it encounters the vortex remaining in the wake from the previous cycle. That wake vortex offers resistance to the new starting vortex motion and acts as a virtual wall in a process termed the wall effect. Ultimately, the starting vortex separates from the bell margin, merging with and largely canceling the previous stopping vortex (Dabiri et al. 2005, 2007). (④) The bell expands outward, and the newly formed stopping vortex gains circulation as it flows inside the subumbrellar cavity. That stopping vortex then generates a high-pressure region that pushes against the subumbrellar surface as passive energy recapture. (⑤) The jellyfish returns to the relaxation phase, and the entire cycle then repeats as it continues swimming.

Passive Energy Recapture

Passive energy recapture contributes significantly to the distance traveled during each propulsive cycle. Following bell contraction, the bell relaxes back to its original conformation. Fluid drawn into the refilling bell is part of a stopping vortex whose rotational flows also generate regions of elevated fluid velocities that push against the inner bell surface (**Figure 7**). This push on the inner surface of the concave bell during refilling contributes a slow but persistent increase in bell motion forward after the bell has completely relaxed, without further energy applied for actuation. Because no further actuation is required for this effect, it is termed a passive process.

PER depends on the medusa harvesting energy contained within the stopping vortex and is completely dependent on the duty cycle of bell contraction. In order to use PER effectively, the medusa must actually pause after bell expansion so that high pressure acting on the subumbrellar surface can slowly push the bell forward and enable the medusa to ride the vortex-generated

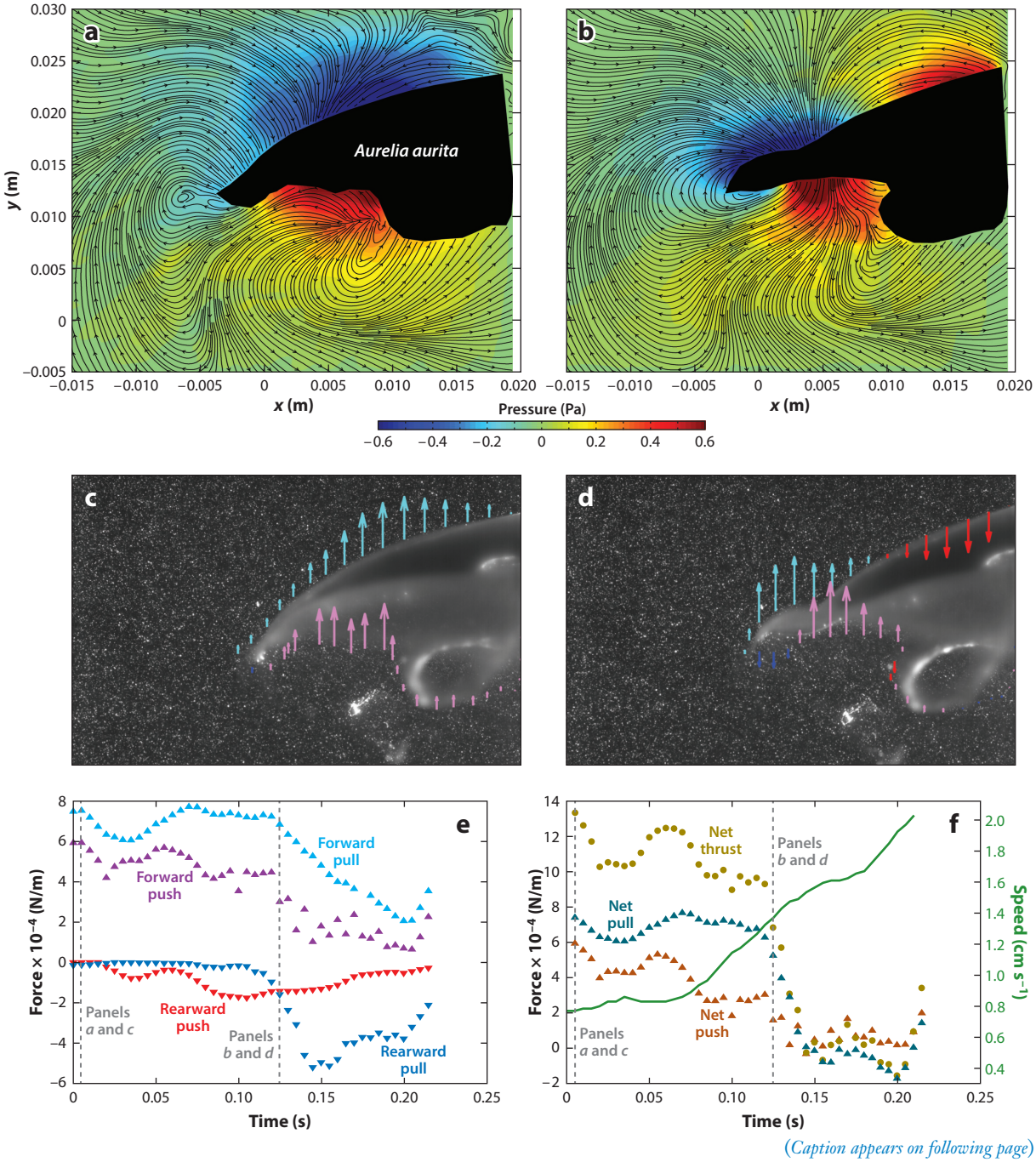

(Caption appears on following page)

Figure 6 (*Figure appears on preceding page*)

Analysis of pressure dynamics during jellyfish (*Aurelia aurita*) linear swimming, illustrating suction thrust. (*a*,*b*) Pressure contours and flow streamlines at two instants during a propulsive swimming stroke. The black shape indicates the left half of the body. (*c*,*d*) Spatial distributions of forward pull (*light blue arrows*), rearward pull (*dark blue arrows*), forward push (*purple arrows*), and rearward push (*red arrows*) due to local fluid pressure. The arrow length is proportional to local pressure magnitude, and the direction indicates the direction of fluid pressure on the body. (*e*) Temporal trends of pressure contributions during a jellyfish propulsive stroke. Vertical lines indicate instants corresponding to data panels as labeled. (*f*) Temporal trends of net pull, net push, and net thrust due to pressure on the body. Vertical lines indicate instants corresponding to data panels as labeled. The speed of the bell apex is indicated by the green curve (*scale at right*). Figure adapted with permission from Gemmell et al. (2015a).

pressure gradient. PER frequently contributes more than a third of the travel distance during a bell pulsation and can make larger contributions when the actuation component of the pulsation cycles is limited to less than 50% (**Figure 8**). Short pulsation cycles that minimize pause periods between contractions allow more rapid animal movement but are less energetically efficient because they minimize the PER contribution (Gemmell et al. 2013, 2018; Hoover et al. 2019; Neil & Askew 2018). Note that PER does not depend on bell shape or size (Gemmell et al. 2018) (**Figure 8*b–d***).

The Virtual Wall Effect

Animals (and machines) swimming or flying near a solid boundary get a boost in performance (Baudinette & Schmidt-Nielsen 1974, Blake 1983, Hainsworth 1988, Nowroozi et al. 2009, Park & Choi 2010, Rayner 1991). The phenomenon of increased lift generated over static surfaces moving parallel to solid boundary is termed the steady wall or steady ground effect. For example, many animals exhibit a reduced cost of transport and improved energetic efficiencies when swimming

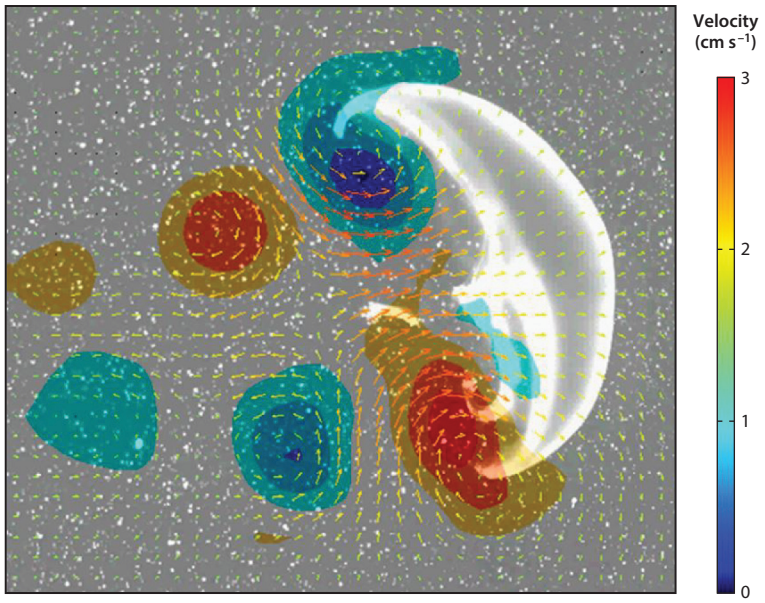

Figure 7

Particle image velocimetry image of the stopping vortex structure during bell refilling by a jellyfish (*Aurelia aurita*). The high-velocity flows in the subumbrellar cavity are the basis of passive energy recapture during bell relaxation. Figure adapted with permission from Gemmell et al. (2013).

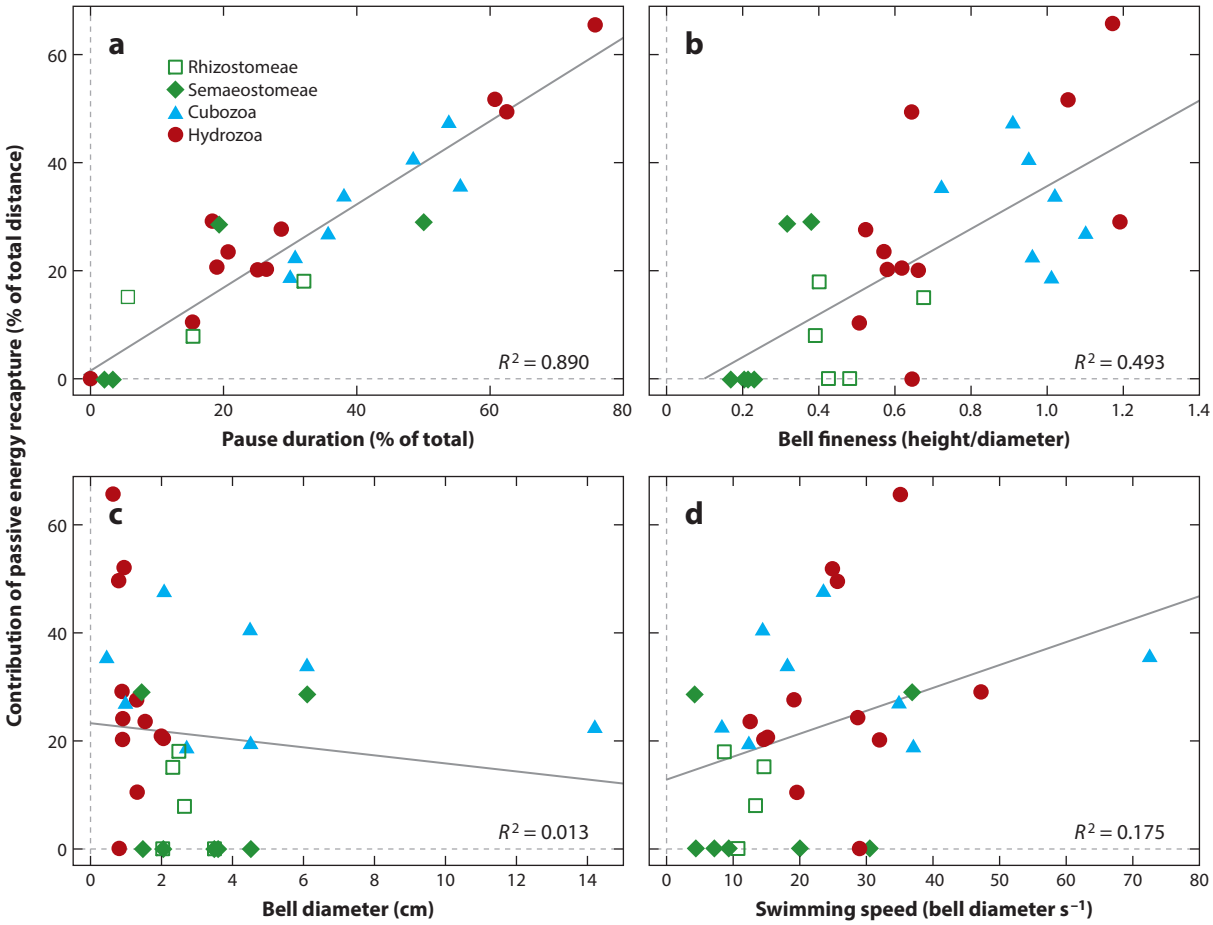

Figure 8

Influence of bell kinematics and morphology on passive energy recapture during medusan swimming. The contribution of passive energy recapture to total travel distance during a contraction–expansion cycle is a function of (*a*) the duration of the pause following bell contraction (as a percentage of total swim cycle duration), (*b*) bell fineness ratio (bell height/bell diameter), (*c*) bell diameter, and (*d*) swimming speed normalized by bell diameter. The solid lines represent linear regressions. Note that only the percentage of the contraction–expansion cycle spent pausing—no bell activity—strongly influences the contribution of passive energy recapture to overall body movement. Figure adapted with permission from Gemmell et al. (2018).

near a wall (Bale et al. 2015, Blake 1979, Liao et al. 2003, Webb 1993), and Fernández-Prats et al. (2015) found considerable propulsive advantages for an undulatory near-wall swimmer, with a 25% increase in speed and 45% increase in thrust near a solid surface. This effect is often modeled as an interaction between a mirrored pair of vortices represented by a true vortex and an opposite-sign virtual vortex on the other side of the wall (Schmid et al. 2009). However, most pelagic animals do not swim near solid surfaces, and consequently, near-body vortex–vortex interactions in open-water swimmers have been poorly investigated.

Examinations using the jellyfish *Aurelia aurita* have clarified the role that vortex interactions can play in animals that swim away from solid boundaries. These studies demonstrated that a vortex ring (stopping vortex) created underneath the animal during the previous swim cycle is critical for increasing propulsive performance (Gemmell et al. 2020) (**Figure 9**). This well-positioned

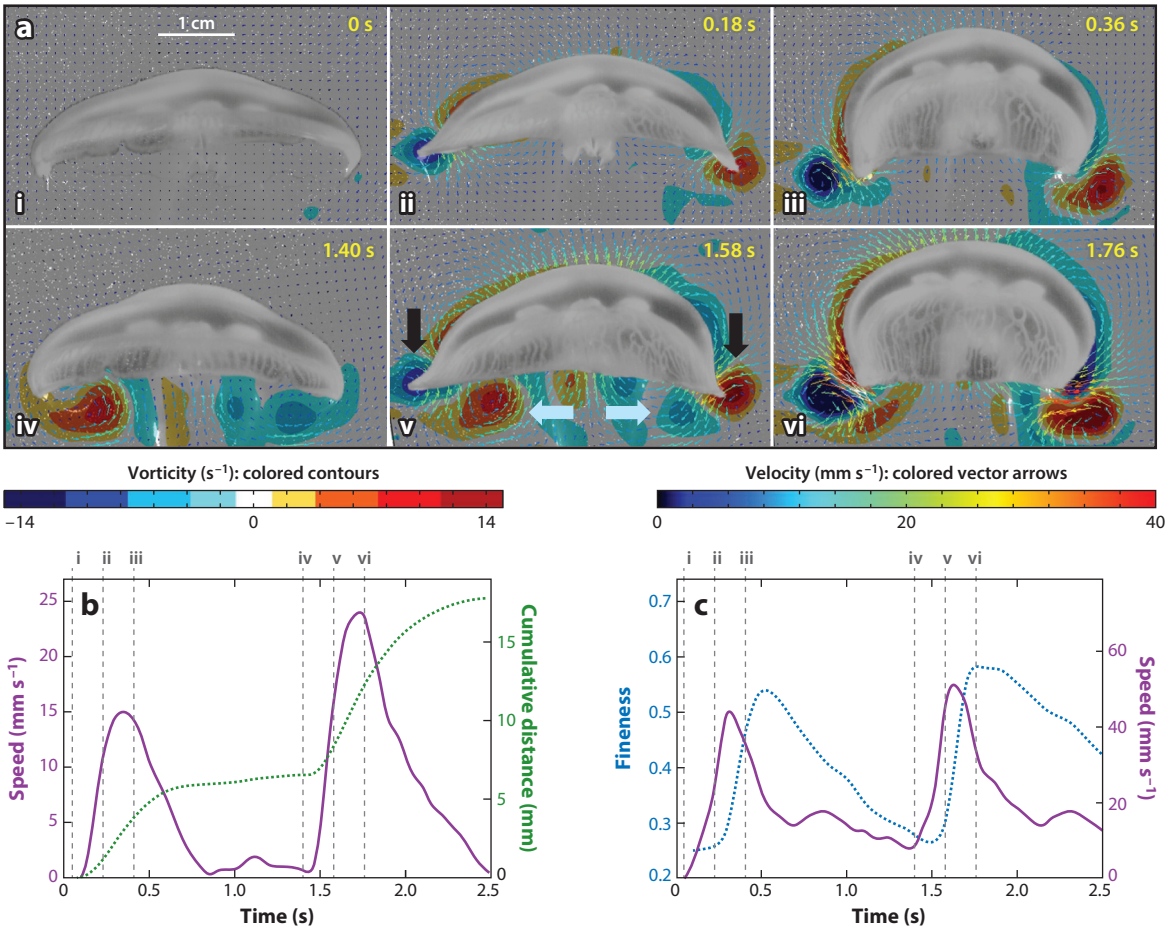

Figure 9

Representative swimming sequence of a 4-cm jellyfish (*Aurelia aurita*) as it begins swimming from rest. (*a*) Fluid vorticity and velocity variables. Note the lack of vorticity under the bell in subpanel *i* and the presence of a stopping vortex prior to the next contraction cycle in subpanel *iv*. Black arrows show an example of the starting vortex, and light blue arrows show the stopping vortex. (*b*,*c*) Kinematic and performance variables during the two swim cycles shown in panel *a*. Vertical gray dashed lines indicate the corresponding subpanels in panel *a*. Panel *b* shows swimming speed (*solid purple line*) and cumulative distance (*dotted green line*); panel *c* shows bell fineness (*dotted blue line*) and the instantaneous speed of the bell margin (*solid purple line*).

stopping vortex acts in the same way as a virtual vortex during wall effect performance enhancement, by helping converge fluid at the underside of the propulsive surface and generating significantly higher pressures that result in greater thrust. Hence, swimming jellyfish serve as a useful model to demonstrate a wall effect boost in open water by creating what amounts to a virtual wall between two real, opposite-sign vortex rings (Gemmell et al. 2020) (**Figure 10**). This contributes to the significant propulsive advantage that jellyfish possess relative to other metazoans and provides a potentially important mechanism to be utilized by bioengineered propulsion systems.

HIGH-EFFICIENCY ROTATION THROUGH FLUIDS

In addition to forward translation, medusae must maneuver, or turn, during swimming. The hydrodynamic sources of the rotational motions required for swimming turns involve principles

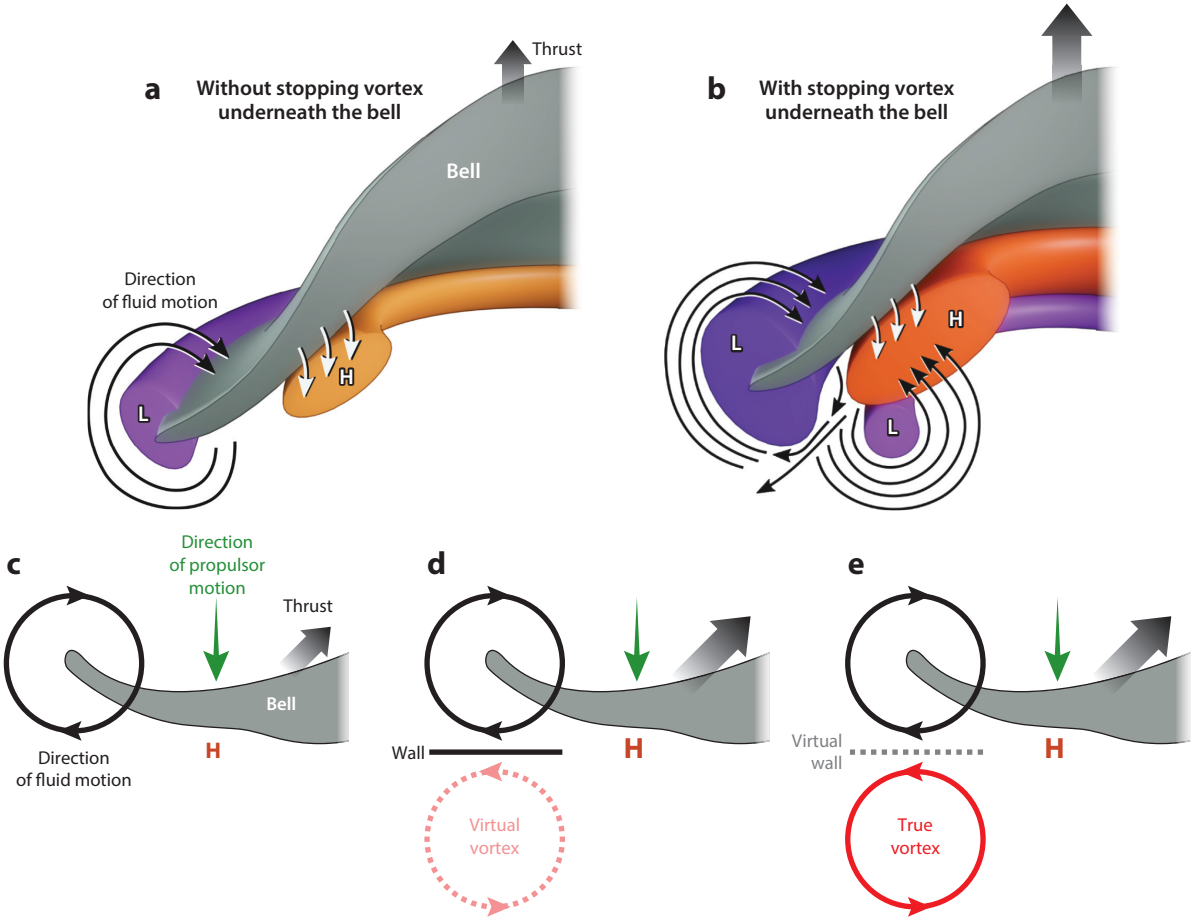

Figure 10

Diagrammatic representations of water movement and pressure anomalies due to the kinematic movement of a jellyfish bell. For simplicity, a cross section through only half of the animal is depicted (*gray surface*). (*a*) Jellyfish swimming without a developed stopping vortex underneath the bell. (*b*) Jellyfish swimming with a developed stopping vortex underneath the bell. In panels *a* and *b*, orange areas denote regions of above-ambient pressure (H), and purple areas denote regions of below-ambient pressure (L). Darker colors represent higher magnitudes of pressure. Black arrows show the direction of fluid motion, white arrows show the direction of movement of the bell margin during the contraction phase, and black gradient arrows depict the relative forward thrust generated. (*c*) Jellyfish swimming in the absence of a solid boundary and without the presence of an additional opposite-sign vortex. (*d*) Wall effect case where swimming near a solid boundary produces an opposite-sign virtual vortex and results in greater positive pressures compared with those in panel *a*. (*e*) Jellyfish swimming in the absence of a solid boundary with a real opposite-sign stopping vortex present. This case represents a jellyfish undergoing routine swimming and results in a virtual wall effect thrust benefit similar to panel *b*. In panels *c*–*e*, green arrows denote the direction of propulsor motion, and black gradient arrows denote relative thrust generation. Panel *d* adapted with permission from Schmid et al. (2009).

that are historically less well considered than translational motions. In contrast to the symmetric bell kinematics characterizing simple straight translation (**Figure 11*a–c***), turning requires body rotation with asymmetric body kinematics and corresponding asymmetric vortex interactions (**Figure 11*d–f***). Both the timing and the spatial kinematics of bell motion are critical for the rotation of the jellyfish during turning. A turn is initiated by the bell margin on the inside of the arc through which the turn will occur. The bell margin to the inside of the turn moves first and

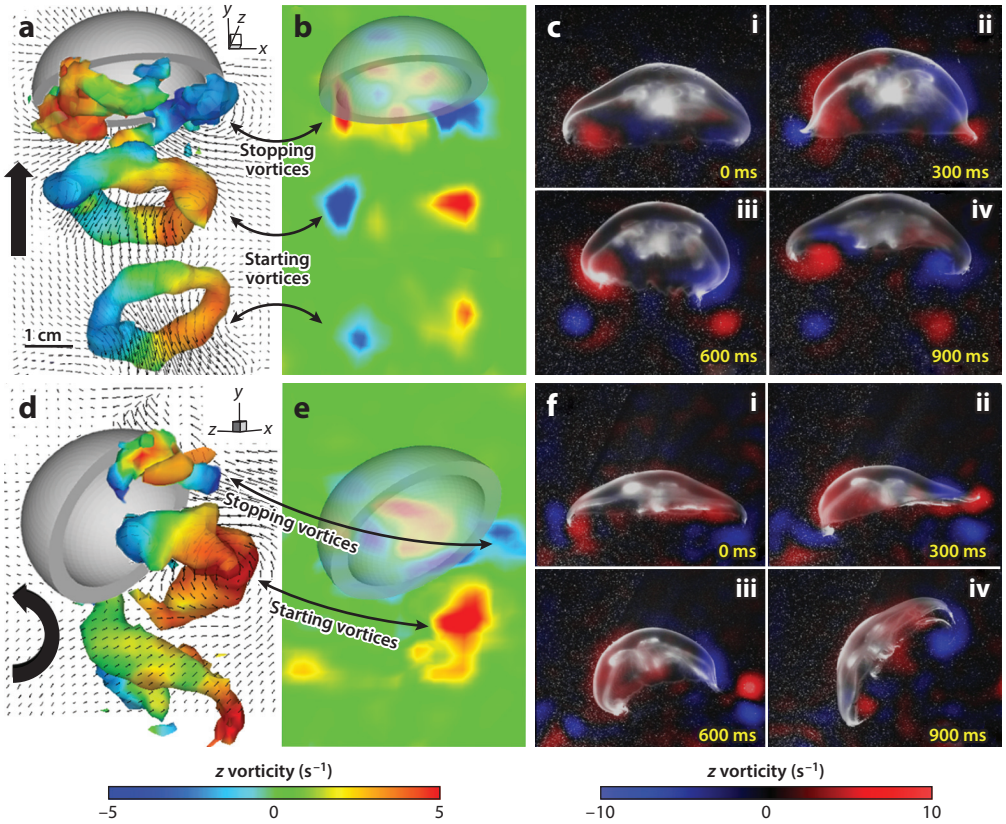

Figure 11

Visualized wakes of a swimming jellyfish (*Aurelia aurita*) performing (*a–c*) straight swimming behavior and (*d–f*) turning behavior. Stopping and starting vortices are indicated. Panels *a* and *d* show the instantaneously captured three-dimensional vorticity produced in the wake of a swimming jellyfish. The gray hemisphere shows the approximate location of the jellyfish. Panels *b* and *e* represent horizontal slices from the sequences shown in panels *a* and *d*, respectively, and are colored using *z* vorticity. Panels *c* and *f* show results from planar particle image velocimetry sequences of straight and turning behavior to illustrate the relationships among body position, kinematics, and vorticity. Figure adapted with permission from Gemmell et al. (2015b).

maintains a comparatively rigid conformation, directing vortex-generated flows toward the bell's central axis (**Figure 11*f*, subpanel *i***). This motion may deter forward motion and establishes a pivot point around which the bell rotates as its central axis changes orientation to the direction of body movement. After the inside margin contraction, the bell margin on the opposite side, or the outside of the turn, undergoes enhanced marginal bending (**Figure 11*f*, subpanel *iii***). This bending produces vortices and flows directed away from the bell and generates torque that pushes the outside of the bell through the arc of the turn. Hence, the inside bell margin establishes a pivot point with restricted travel distance, while the outside bell margin travels through a larger arc. Extreme turns entail both pronounced temporal and conformational differences in bell margin kinematics, but a series of more gradual asymmetric contraction cycles can achieve less dramatic turns and allows for minor course adjustments.

Noninvasive optical methods have recently clarified interactions between torque generation and the jellyfish body's moment of inertia during these turning motions. Asymmetric body motions (**Figure 12*a–d***) create pronounced alterations in the pressure fields in the water adjacent to

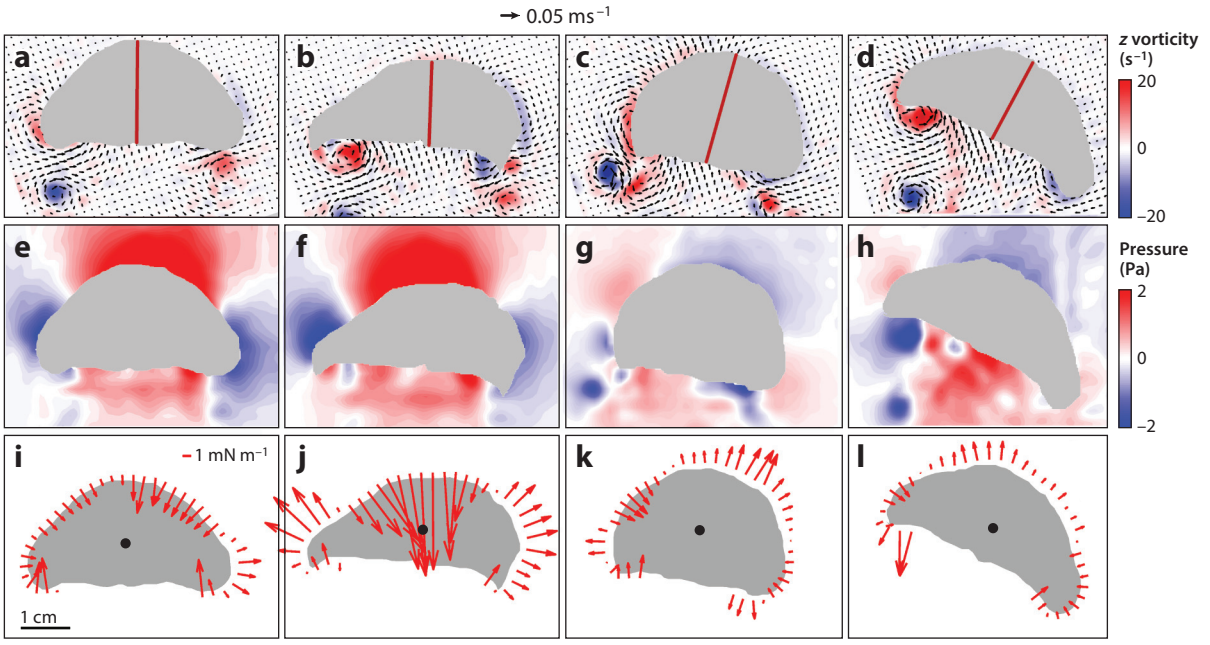

Figure 12

Turning kinematics and fluid pressure for a representative jellyfish (*Aurelia aurita*) turn (30° rotation). (*a–d*) Particle image velocimetry vector and vorticity fields. The red line shows the midline of the medusa throughout the turn. (*e–h*) Pressure fields around the medusa. The jellyfish generates large, asymmetric pressure gradients around its body (panel *f*) before major body orientation shifts (illustrated by the midline position). (*i–l*) Force vectors due to local fluid pressure at the jellyfish body surface (*red arrows*). Turning involves strong torque forces at bell margins with simultaneous stabilization of the central body disc (panel *j*). This combination allows the bell margins to rotate around the central axis of the jellyfish bell during a turn. Figure adapted with permission from Dabiri et al. (2019).

the animal (**Figure 12*e–h***). The largest pressure field alterations (**Figure 12*f***) precede the more pronounced bell contraction that occurs during the subsequent turn. The majority of body axis rotation during the turn occurs after the maximum torque application (**Figure 12*j–l***).

Examination of jellyfish body kinematics during the period of transient pressure buildup led to the discovery of a small, rapid shift in the curvature of the animal body immediately preceding the turn (1.5% ± 1.0% change in curvature; for details, see Dabiri et al. 2019). Although the amplitude of this initial body bend was small, it occurred over a sufficiently short period of time—a few milliseconds—that the corresponding acceleration of the body was large relative to accelerations during unidirectional translational swimming. This motion was transmitted to the adjacent water via a process known as the acceleration reaction or added-mass effect (Daniel 1984). Because water is effectively incompressible, the fluid in contact with the body responded to the high local body acceleration by an increase in the local fluid pressure where the body was advancing (pushing the water) and a decrease in the local pressure where the body surface retreated from the local water (pulling the water with it). When integrated over the full animal body, the pressure field created by the small, asymmetric body bending results in a large net torque capable of turning the organism toward a new heading. The more pronounced body motions that occur after the generation of this pressure field do not contribute greatly to torque generation, but they do reduce the moment of inertia of the body. Therefore, the body kinematics that follow peak pressure generation enhance the effect of the generated torque by amplifying the resulting angular acceleration so that the body rotates rapidly through a turn. Although the maximum torque generation and minimum moment

of inertia do not occur simultaneously, the inertia of the fluid and of the animal body allows the initial pressure transient to affect subsequent turning dynamics.

Rotational dynamics: the modulation of turning by fine-tuning of the timing and spatial kinematics of bell motion

The ultimate magnitude of each turning maneuver is modulated by changes in body shape that tune the moment of inertia and thereby control the angular acceleration of the body. An essential requirement for these rotational dynamics is body flexibility (**Figures 11** and **12**), which enables the jellyfish to dynamically redistribute its mass and manipulate the lever arm of the propulsive surfaces used to initiate the turn (e.g., the bell margin of the jellyfish) and the body moment of inertia. While we have described rotational dynamics for the jellyfish *Aurelia aurita*, the performance advantages of this turning strategy may select for very similar turning kinematics by other animal swimmers and could potentially be used in biomimetic vehicles (Dabiri et al. 2019).

CONCLUSIONS

Jellyfish overcame the phylogenetic constraints shared with other cnidarians by capitalizing on fundamental hydrodynamic interactions that enable successful propulsion and maneuvering using comparatively simple body designs and low force production. Studies of jellyfish swimming have contributed to understanding of animal swimming in general because solutions such as suction thrust (Gemmell et al. 2015a) and turning dynamics (J.O. Dabiri, S.P. Colin, B.J. Gemmell, K.N. Lucas, M. Leftwich & J.H. Costello, manuscript in review) also apply to many other animals.

The same constraints acting on jellyfish swimming may also serve as assets in engineered vehicle design (Yu et al. 2016). Limited material and neural complexity, low force production, and high propulsive efficiency are favorable vehicle design parameters embodied by jellyfish swimmers. It remains important to remember, however, that the apparent simplicity of jellyfish propulsion belies complexities, such as propulsor flexibility and vortex manipulation, which are not easily replicated within the current conventions of human engineering. Fortunately, the ease of laboratory maintenance and research with jellyfish may support future mastery of these principles.

SUMMARY POINTS

1. Jellyfish (cnidarian scyphomedusae) are among the most energetically efficient swimmers of all animals.
2. The relative ease of laboratory experimentation and the axisymmetry and transparent tissues of jellyfish make them ideal models for studying the kinematics and fluid mechanics of swimming.
3. Force production during jellyfish swimming is strongly constrained because of their simple morphology and a muscle fiber arrangement that is limited to one cell layer.
4. Pulsatile swimming with a flexible bell margin creates vortex rings. The interaction of these vortices gives rise to several novel fluid mechanical phenomena that were discovered in jellyfish and had not been previously described. These phenomena explain the energetic efficiency of jellyfish.
5. All of the above-mentioned features make jellyfish useful models to inform the engineering of biomimetic swimming vehicles.

FUTURE ISSUES

1. Although some species of jellyfish are amenable to laboratory measurements, developments in field-based measurements will increase the capacity to study the more fragile forms in the natural environment and to track individuals during long-distance migrations.
2. Comparative studies across aquatic swimmers will allow us to determine the extent to which propulsive principles leveraged by cnidarian medusae appear in other phyla.
3. Our detailed understanding of the principles governing effective swimming in jellyfish has reached a point where we can apply these principles to vehicle design.

DISCLOSURE STATEMENT

The authors are not aware of any affiliations, memberships, funding, or financial holdings that might be perceived as affecting the objectivity of this review.

ACKNOWLEDGMENTS

We thank the numerous colleagues working at the interface of biology and physics for productive conversations on this topic. We are grateful to an anonymous reviewer and the editorial staff at Annual Reviews for improving the article. Funding was provided by the Gordon and Betty Moore Foundation (8835), the National Science Foundation (1511721, 1536672) and the Office of Naval Research (N68335-19-C-0303).

LITERATURE CITED

Alexander RM. 2003. *Principles of Animal Locomotion*. Princeton, NJ: Princeton Univ. Press

Anderson PA, Schwab WE. 1981. The organization and structure of nerve and muscle in the jellyfish *Cyanea capillata* (Coelenterata; Scyphozoa). *J. Morphol.* 170:383–99

Bale R, Neveln ID, Bhalla APS, MacIver MA, Patankar NA. 2015. Convergent evolution of mechanically optimal locomotion in aquatic invertebrates and vertebrates. *PLOS Biol.* 13:e1002123

Baudinette R, Schmidt-Nielsen K. 1974. Energy cost of gliding flight in herring gulls. *Nature* 248:83–84

Biewener A, Patek S. 2018. *Animal Locomotion*. Oxford, UK: Oxford Univ. Press

Blake R. 1979. The energetics of hovering in the mandarin fish (*Synchropus picturatus*). *J. Exp. Biol.* 82:25–33

Blake R. 1983. Mechanics of gliding in birds with special reference to the influence of the ground effect. *J. Biomech.* 16:649–54

Boelsterli U. 1977. An electron microscopic study of early developmental stages, myogenesis, oogenesis and cnidogenesis in the anthomedusa, *Podocoryne carnea* M. Sars. *J. Morphol.* 154:259–89

Bone Q, Trueman E. 1982. Jet propulsion of the calycophoran siphonophores *Chelophyes* and *Abylopsis*. *J. Mar. Biol. Assoc. UK* 62:263–76

Bonner JT. 1965. *Size and Cycles: An Essay on the Structure of Biology*. Princeton, NJ: Princeton Univ. Press

Chapman DM. 1974. *Cnidarian Histology*. New York: Academic

Colin SP, Costello JH, Dabiri JO, Villanueva A, Blottman JB, et al. 2012. Biomimetic and live medusae reveal the mechanistic advantages of a flexible bell margin. *PLOS ONE* 7:e48909

Collins AG, Schuchert P, Marques AC, Jankowski T, Medina M, Schierwater B. 2006. Medusozoan phylogeny and character evolution clarified by new large and small subunit rDNA data and an assessment of the utility of phylogenetic mixture models. *Syst. Biol.* 55:97–115

Costello JH, Colin SP, Dabiri JO. 2008. Medusan morphospace: phylogenetic constraints, biomechanical solutions, and ecological consequences. *Invertebr. Biol.* 127:265–90

Costello JH, Colin SP, Gemmell BJ, Dabiri JO. 2019. Hydrodynamics of vortex generation during bell contraction by the hydromedusa *Eutonina indicans* (Romanes, 1876). *Biomimetics* 4:44

Dabiri JO, Bose S, Gemmell BJ, Colin SP, Costello JH. 2014. An algorithm to estimate unsteady and quasi-steady pressure fields from velocity field measurements. *J. Exp. Biol.* 217:331–36

Dabiri JO, Colin SP, Costello JH. 2006. Fast-swimming hydromedusae exploit velar kinematics to form an optimal vortex wake. *J. Exp. Biol.* 209:2025–33

Dabiri JO, Colin SP, Costello JH. 2007. Morphological diversity of medusan lineages constrained by animal–fluid interactions. *J. Exp. Biol.* 210:1868–73

Dabiri JO, Colin SP, Costello JH, Gharib M. 2005. Flow patterns generated by oblate medusan jellyfish: field measurements and laboratory analyses. *J. Exp. Biol.* 208:1257–65

Dabiri JO, Colin SP, Gemmell BJ, Lucas KN, Leftwich M, Costello JH. 2019. Primitive and modern swimmers solve the challenges of turning similarly to achieve high maneuverability. bioRxiv 706762. **https://doi.org/10.1101/706762**

Daniel TL. 1983. Mechanics and energetics of medusan jet propulsion. *Can. J. Zool.* 61:1406–20

Daniel TL. 1984. Unsteady aspects of aquatic locomotion. *Am. Zool.* 24:121–34

DeMont ME, Gosline JM. 1988a. Mechanics of jet propulsion in the hydromedusan jellyfish, *Polyorchis pexicillatus*: I. Mechanical properties of the locomotor structure. *J. Exp. Biol.* 134:313–32

DeMont ME, Gosline JM. 1988b. Mechanics of jet propulsion in the hydromedusan jellyfish, *Polyorchis penicillatus*: II. Energetics of the jet cycle. *J. Exp. Biol.* 134:333–45

Drucker EG, Lauder GV. 2000. A hydrodynamic analysis of fish swimming speed: wake structure and locomotor force in slow and fast labriform swimmers. *J. Exp. Biol.* 203:2379–93

Dular M, Bajcar T, Širok B. 2009. Numerical investigation of flow in the vicinity of a swimming jellyfish. *Eng. Appl. Comput. Fluid Mech.* 3:258–70

Feitl K, Millett A, Colin SP, Dabiri JO, Costello JH. 2009. Functional morphology and fluid interactions during early development of the scyphomedusa *Aurelia aurita*. *Biol. Bull.* 217:283–91

Fernández-Prats R, Raspa V, Thiria B, Huera-Huarte F, Godoy-Diana R. 2015. Large-amplitude undulatory swimming near a wall. *Bioinspir. Biomim.* 10:016003

Fish FE, Lauder GV. 2017. Control surfaces of aquatic vertebrates: active and passive design and function. *J. Exp. Biol.* 220:4351–63

Floryan D, Van Buren T, Smits AJ. 2019. Swimmers' wakes are not reliable indicators of swimming performance. arXiv:1906.10826 [physics.flu-dyn]

Frame J, Lopez N, Curet O, Engeberg ED. 2018. Thrust force characterization of free-swimming soft robotic jellyfish. *Bioinspir. Biomim.* 13:064001

Gemmell BJ, Colin SP, Costello JH. 2018. Widespread utilization of passive energy recapture in swimming medusae. *J. Exp. Biol.* 221:jeb168575

Gemmell BJ, Colin SP, Costello JH, Dabiri JO. 2015a. Suction-based propulsion as a basis for efficient animal swimming. *Nat. Commun.* 6:8790

Gemmell BJ, Costello JH, Colin SP, Stewart CJ, Dabiri JO, et al. 2013. Passive energy recapture in jellyfish contributes to propulsive advantage over other metazoans. *PNAS* 110:17904–9

Gemmell BJ, Du Clos KT, Colin SP, Sutherland KR, Costello JH. 2020. The most efficient metazoan swimmer creates a 'virtual wall' to enhance performance. bioRxiv 2020.05.01.069518. **https://doi.org/10.1101/2020.05.01.069518**

Gemmell BJ, Troolin DR, Costello JH, Colin SP, Satterlie RA. 2015b. Control of vortex rings for manoeuvrability. *J. R. Soc. Interface* 12:20150389

Gladfelter W. 1972. Structure and function of the locomotory system of the Scyphomedusa *Cyanea capillata*. *Mar. Biol.* 14:150–60

Gladfelter W. 1973. A comparative analysis of the locomotory systems of medusoid Cnidaria. *Helgol. Wiss. Meeresunters.* 25:228–72

Hainsworth FR. 1988. Induced drag savings from ground effect and formation flight in brown pelicans. *J. Exp. Biol.* 135:431–44

Higgins J III, Ford M, Costello JH. 2008. Transitions in morphology, nematocyst distribution, fluid motions, and prey capture during development of the scyphomedusa *Cyanea capillata*. *Biol. Bull*. 214:29–41
Hoover AP, Griffith BE, Miller LA. 2017. Quantifying performance in the medusan mechanospace with an actively swimming three-dimensional jellyfish model. *J. Fluid Mech.* 813:1112–55
Hoover AP, Porras AJ, Miller LA. 2019. Pump or coast: the role of resonance and passive energy recapture in medusan swimming performance. *J. Fluid Mech.* 863:1031–61
Joshi A, Kulkarni A, Tadesse Y. 2019. FludoJelly: experimental study on jellyfish-like soft robot enabled by soft pneumatic composite (SPC). *Robotics* 8:56
Jusufi A, Vogt DM, Wood RJ, Lauder GV. 2017. Undulatory swimming performance and body stiffness modulation in a soft robotic fish-inspired physical model. *Soft Robot*. 4:202–10
Kim H-S, Lee J-Y, Chu W-S, Ahn S-H. 2017. Design and fabrication of soft morphing ray propulsor: undulator and oscillator. *Soft Robot*. 4:49–60
Liao JC, Beal DN, Lauder GV, Triantafyllou MS. 2003. Fish exploiting vortices decrease muscle activity. *Science* 302:1566–69
Lipinski D, Mohseni K. 2009. Flow structures and fluid transport for the hydromedusae *Sarsia tubulosa* and *Aequorea victoria*. *J. Exp. Biol*. 212:2436–47
Lucas KN, Dabiri JO, Lauder GV. 2017. A pressure-based force and torque prediction technique for the study of fish-like swimming. *PLOS ONE* 12:e0189225
McHenry MJ. 2007. Comparative biomechanics: the jellyfish paradox resolved. *Curr. Biol.* 17:R632–33
McHenry MJ, Jed J. 2003. The ontogenetic scaling of hydrodynamics and swimming performance in jellyfish (*Aurelia aurita*). *J. Exp. Biol.* 206:4125–37
Megill WM, Gosline JM, Blake RW. 2005. The modulus of elasticity of fibrillin-containing elastic fibres in the mesoglea of the hydromedusa *Polyorchis penicillatus*. *J. Exp. Biol*. 208:3819–34
Miles JG, Battista NA. 2019. Naut your everyday jellyfish model: exploring how tentacles and oral arms impact locomotion. *Fluids* 4:169
Nagata RM, Morandini AC, Colin SP, Migotto AE, Costello JH. 2016. Transitions in morphologies, fluid regimes, and feeding mechanisms during development of the medusa *Lychnorhiza lucerna*. *Mar. Ecol. Prog. Ser*. 557:145–59
Najem J, Sarles SA, Akle B, Leo DJ. 2012. Biomimetic jellyfish-inspired underwater vehicle actuated by ionic polymer metal composite actuators. *Smart Mater. Struct.* 21:094026
Nawroth JC, Feitl K, Colin SP, Costello JH, Dabiri JO. 2010. Phenotypic plasticity in juvenile jellyfish medusae facilitates effective animal–fluid interaction. *Biol. Lett.* 6:389–93
Nawroth JC, Lee H, Feinberg AW, Ripplinger CM, McCain ML, et al. 2012. A tissue-engineered jellyfish with biomimetic propulsion. *Nat. Biotechnol.* 30:792
Neil TR, Askew GN. 2018. Jet-paddling jellies: swimming performance in the Rhizostomeae jellyfish *Catostylus mosaicus*. *J. Exp. Biol*. 221:jeb191148
Nowroozi BN, Strother JA, Horton JM, Summers AP, Brainerd EL. 2009. Whole-body lift and ground effect during pectoral fin locomotion in the northern spearnose poacher (*Agonopsis vulsa*). *Zoology* 112:393–402
O'Dor R, Hoar J. 2000. Does geometry limit squid growth? *ICES J. Mar. Sci.* 57:8–14
Park H, Choi H. 2010. Aerodynamic characteristics of flying fish in gliding flight. *J. Exp. Biol.* 213:3269–79
Park SG, Chang CB, Huang W-X, Sung HJ. 2014. Simulation of swimming oblate jellyfish with a paddling-based locomotion. *J. Fluid Mech*. 748:731–55
Pauly D. 1997. Geometrical constraints on body size. *Trends Ecol. Evol.* 12:442
Quinn DB, Lauder GV, Smits AJ. 2014. Scaling the propulsive performance of heaving flexible panels. *J. Fluid Mech*. 738:250–67
Rayner JM. 1991. On the aerodynamics of animal flight in ground effect. *Philos. Trans. R. Soc. Lond. B* 334:119–28
Ren Z, Hu W, Dong X, Sitti M. 2019. Multi-functional soft-bodied jellyfish-like swimming. *Nat. Commun.* 10:2703
Ruiz LA, Whittlesey RW, Dabiri JO. 2011. Vortex-enhanced propulsion. *J. Fluid Mech*. 668:5–32
Satterlie RA. 2002. Neuronal control of swimming in jellyfish: a comparative story. *Can. J. Zool.* 80:1654–69
Satterlie RA. 2011. Do jellyfish have central nervous systems? *J. Exp. Biol.* 214:1215–23

Satterlie RA. 2015. The search for ancestral nervous systems: an integrative and comparative approach. *J. Exp. Biol.* 218:612–17

Schmid S, Lutz T, Krämer E. 2009. Impact of modelling approaches on the prediction of ground effect aerodynamics. *Eng. Appl. Comput. Fluid Mech.* 3:419–29

Schuchert P, Reber-Müller S, Schmid V. 1993. Life stage specific expression of a myosin heavy chain in the hydrozoan *Podocoryne carnea*. *Differentiation* 54:11–18

Seipel K, Schmid V. 2005. Evolution of striated muscle: jellyfish and the origin of triploblasty. *Dev. Biol.* 282:14–26

Simmons SL, Satterlie RA. 2018. Tentacle musculature in the cubozoan jellyfish *Carybdea marsupialis*. *Biol. Bull.* 235:91–101

Tytell ED, Lauder GV. 2004. The hydrodynamics of eel swimming: I. Wake structure. *J. Exp. Biol.* 207:1825–41

Villanueva A, Bresser S, Chung S, Tadesse Y, Priya S. 2009. Jellyfish inspired underwater unmanned vehicle. In *Electroactive Polymer Actuators and Devices (EAPAD) 2009*, ed. Y Bar-Cohen, T Wallmersperger, pp. 458–69. Proc. SPIE 7287. Bellingham, WA: Soc. Photo-Opt. Instrum. Eng.

Villanueva A, Smith C, Priya S. 2011. A biomimetic robotic jellyfish (Robojelly) actuated by shape memory alloy composite actuators. *Bioinspir. Biomim.* 6:036004

Vogel S. 2013. *Comparative Biomechanics: Life's Physical World*. Princeton, NJ: Princeton Univ. Press

Webb PW. 1993. The effect of solid and porous channel walls on steady swimming of steelhead trout *Oncorhynchus mykiss*. *J. Exp. Biol.* 178:97–108

Whittlesey RW, Dabiri JO. 2013. Optimal vortex formation in a self-propelled vehicle. *J. Fluid Mech.* 737:78–104

Willert CE, Gharib M. 1991. Digital particle image velocimetry. *Exp. Fluids* 10:181–93

Xu NW, Dabiri JO. 2020. Low-power microelectronics embedded in live jellyfish enhance propulsion. *Sci. Adv.* 6:eaaz3194

Yu J, Li X, Pang L, Wu Z. 2019. Design and attitude control of a novel robotic jellyfish capable of 3D motion. *Sci. China Inf. Sci.* 62:194201

Yu J, Xiao J, Li X, Wang W. 2016. Towards a miniature self-propelled jellyfish-like swimming robot. *Int. J. Adv. Robot. Syst.* 13(5). **https://doi.org/10.1177/1729881416666796**

Zimmerman KL, Jamshidi AD, Buckenberger A, Satterlie RA. 2019. Organization of the subumbrellar musculature in the ephyra, juvenile, and adult stages of *Aurelia aurita* Medusae. *Invertebr. Biol.* 138:e12260

RELATED RESOURCES

Free software for estimating pressure field from velocity field measurements: **http://dabirilab.com/software**

Free software for calculating force and torque from pressure field measurements: **https://github.com/kelseynlucas/Aurelia-force-and-torque**